

Basic investigation on a robust and practical plant diagnostic system

Erika Fujita, Yusuke Kawasaki
*Applied Informatics,
 Graduate School of
 Science and Engineering,
 Hosei University, Japan*

Hiroyuki Uga
*Saitama Agricultural
 Technology Research
 Center, Japan*

Satoshi Kagiwada
*Clinical Plant Science,
 Faculty of Bioscience
 and Applied Chemistry,
 Hosei University, Japan*

Hitoshi Iyatomi
*Applied Informatics,
 Graduate School of
 Science and Engineering,
 Hosei University, Japan*

Abstract—Accurate plant diagnosis requires experts’ knowledge but is usually expensive and time consuming. Therefore, it has become necessary to design an accurate, easy, and low-cost automated diagnostic system for plant diseases. In this paper, we propose a new practical plant-disease detection system. We use 7,520 cucumber leaf images comprising images of healthy leaves and those infected by almost all types of viral diseases. The leaves were photographed on site under only one requirement, that is, each image must contain a leaf roughly at its center, thus providing them with a large variety of appearances (i.e., parameters including distance, angle, background, and lighting condition were not uniform). Although half of the images used in this experiment were taken in bad conditions, our classification system based on convolutional neural networks attained an average of 82.3% accuracy under the 4-fold cross validation strategy.

Keywords—deep learning; plant disease; convolutional neural networks;

I. INTRODUCTION

Plant diseases critically affect agricultural production [1]. To minimize the damage, we must determine and implement appropriate countermeasures immediately. Especially, viral plant diseases have no treatment and spread with disease vector rapidly; thus, infected plants must be removed immediately to avoid secondary infections. First, experts usually conduct diagnosis of plants through visual examination; however, they may sometimes miss or misdiagnose because of the wide varieties of disease symptoms. Genetic testing is conducted if needed but it is expensive and time consuming.

Therefore, accurate, easy, and low-cost automated plant diagnosis is required from agricultural industries. Several studies have investigated automated plant diagnosis by using machine-learning methods [2]–[7]. Pujari et al. used neural networks to classify fungal diseases and showed 87.8% in accuracy [2]. Yao et al. used support vector machines to classify rice-plant disease and attained 92.7% accuracy [3]. However, the aforementioned procedures face difficulty in detecting regions of interest (ROIs) for subsequent processing (e.g., segmenting out the pathological changes from surrounding leaflets in images) and in designing and implementing efficient diagnosis parameter feeds to classifiers.

In recent years, new machine-learning schema called deep learning has been widely noticed as one of the most

promising techniques for intelligent information processing. Convolutional Neural Networks (CNNs) are a principal component of deep learning specialized for image recognition or so-called computer vision. CNNs automatically obtain efficient image features for classification from the training images as part of their learning process and attain high classification performance [8], thus significantly reducing the need for the abovementioned complexities.

Sharada et al. trained CNNs with Plant Village dataset [9] and obtained the highest classification accuracy of 99.35% [10]. Although the Plant Village dataset has wide variety of leaf images of crops and their diseases, the photographs were obtained after being cropped for each leaf, and they were in almost ideal conditions, that is, uniform lighting, distance, angle, and backgrounds. Thus, they showed the applicability of CNNs in diagnosing plant diseases, while there is still scope for further investigations for the development of a practical system. Before their proposal, the objective of our research was to develop a practical and versatile automated plant diagnostic system, and we built a prototype with CNNs [11]. We targeted cucumber because it is a very common product among crops [12] and we have the required expertise. We designed our system to be accurate and easily available on site. Further, we had only one requirement for collecting images for the system: each image should contain a leaf roughly at its center. Images were thus obtained, and accordingly they had large variety of appearances (i.e., distance, angle, background, and lighting conditions were not uniform). This mild regulation was due to our expectation that the input of our system would be given the picture photographed by smartphones or similar consumer devices on site. This obviously made it difficult to follow the classification steps. In our previous research, we attained 94.9% accuracy in discriminating healthy cucumbers from among those affected by two types of viral diseases by using the 4-fold cross validation strategy. This result demonstrated that a practical onsite diagnosis of plant disease is within reach. However, in terms of practical application, the types of disease supported by the system were limited. In this study, we developed a new diagnostic system for diagnosing almost all range (seven types) of viral diseases that cucumbers can be infected with. The dataset

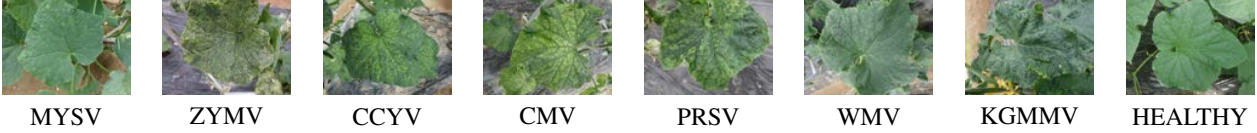


Figure 1. The seven types of diseases and healthy

contains half of the bad-condition images, such as highlights or shadows observed in leaves, which sometimes saturate the capable range of camera sensitivity. This is because they might be frequently occurred on site, and our objective is to develop a robust and practical system rather than just pursuing numerical diagnostic accuracy.

II. METHOD

A. Datasets

We created two types of datasets (Dataset-1 and 2) consisting of cucumber leaf images supplied from Saitama Agricultural Technology Research Center, Japan. The images were photographed using a commonly available digital camera onsite and each image contains a leaf roughly at its center. The datasets cover healthy cucumber plants and those with all the viral diseases, as a matter of practice (melon yellow spot virus: MYSV, zucchini yellow mosaic virus: ZYMV, cucurbit clorotic yellows virus: CCYV, cucumber mosaic virus: CMV, papaya ring spot virus: PRSV, watermelon mosaic virus: WMV, and kyuri (=cucumber) green mottle mosaic virus: KGMMV). Figure 1 illustrates the seven types of diseases and healthy in the cucumber plant. Dataset-1 consists of 7,320 cucumber leaf images (CMV: 320; and all other classes: 1,000). All images in this dataset were taken under relatively good conditions, shown in Figure 1. Dataset-2 consists of 7,520 cucumber leaf images (MYSV: 1,000, ZYMV: 1,000, CCYV: 1,000, CMV: 720, PRSV: 880, WMV: 780, KGMMV: 840, and healthy: 1,300). In this dataset, the ratio of “good-condition” images (as in Figure 1) to “bad-condition” images (as shown in Figure 2) is 1:1 for each class. Owing to restrictions of available images, the number of cases in each class does not match. In particular, CMV-affected leaves hardly show their symptoms because of their attributes; therefore, the number of cases is limited.



Figure 2. Examples of bad-condition image in Dataset-2

B. Preprocessing and data augmentation

Data augmentation [8], [13], [14] is commonly used to improve the generality of the classifier, especially if the amount of training data given is limited. In this study, we

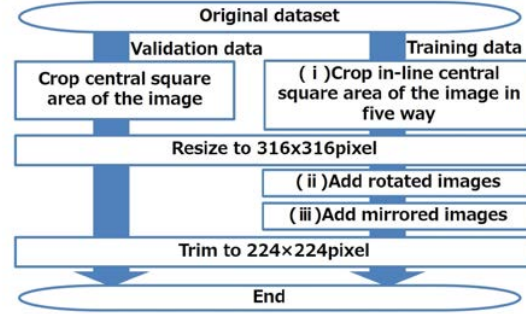


Figure 3. Outline of preprocessing

introduced three types of data augmentations, namely (i) image shifting, (ii) image rotation, and (iii) image mirroring in this study. Note that we used image rotation in our previous study [11] and confirmed its significant contributions. To realize the earlier augmentation methods considering their practical application, we preprocessed the images, as shown in Figure 3. For each training image, (i) we first cropped it to a square with side length equal to that of the short side of the original image. Simultaneously, we chose inline five areas with a certain stride size, and these five images are resized to 316×316 pixels. This is larger than the actual input size for the CNNs (224×224 pixels) for the appropriate working of the following image rotation, that is, to avoid running off the edge of each image. This augmentation increases the size of the training data to five times. (ii) Next, we rotated the image with 10° increment and cropped each center with 224×224 pixels size (increases data $\times 36$). (iii) Finally, we generate mirror images with respect to horizontal axes of the images (increases data $\times 2$).

Overall, our data augmentation artificially increases the training data to 360 times its original size.

C. Architecture

The CNNs of our system consists of an input layer; convolution layers, which perform convolution, pooling, and local response normalization (LRN) operations; and an output layer. The input layer takes a 224×224 pixels RGB image. The output comprises a class with the maximum a posterior probability given by the softmax function at the output layer. As our task consists of an eight-class classification problem (i.e., seven diseased and one healthy plant), the number of nodes in the output layer is eight. Figure 4 show the proposed CNN’s architecture. The parameters of LRN were set the same as those in AlexNet [8]. This configuration was determined based on our preliminary experiments and

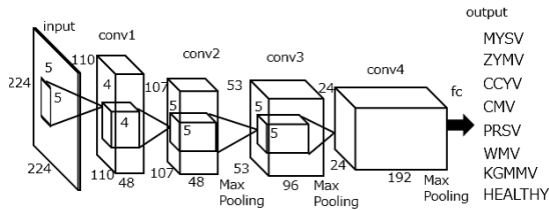


Figure 4. Proposed CNNs architecture

VGG Net [15]. Our CNNs was developed using “Caffe” frameworks [16].

D. Experiments

In this study, we used two CNNs: CNN-1 and CNN-2 to train Dataset-1 and Dataset-2, respectively. Here, these two CNNs architectures are same settings. In addition, we compared the diagnostic performance of the CNNs for good- and bad-condition images with different data augmentation settings. Next, we evaluated these CNNs with good- and bad-condition images, respectively.

For evaluation criteria, we calculated sensitivity and specificity for each disease. Specificity is equal to sensitivity for healthy plant and the accuracy indicates the average among all sensitivity and specificity values. Basically, evaluations were performed under the 4-fold cross validation strategy. To evaluate CNN-1 with bad-condition images, we used bad-condition images in Dataset-2.

III. RESULTS

Table I summarizes the diagnostic performance for good- and bad-condition images of CNN-1 and CNN-2, respectively. Figure 5 illustrates images in which CNN-2 diagnosed correctly but CNN-1 misdiagnosed. Table II summarizes the results of diagnostic performances of CNN-1 and 2 by using different data augmentation methods. Note that CNN-1 trained using only good-condition images in each experiments.

IV. DISCUSSION

Table I shows an almost equivalent diagnostic performance (82%-83%) between the two CNNs. It is interesting

that CNN-1 did not outperform CNN-2 significantly, even though it has trained and tested only ideally obtained images. Table I shows that although CNN-2 showed some strong and weak points, it is almost equivalent in diagnosing both good- and bad-condition images on an average, whereas CNN-1 is not.

The diagnostic performance of CNN-1 (trained using Dataset-1; only good-condition images) was improved due to the introduction of data augmentation procedures (see Table II). In this study, a wide variety of disease symptoms were observed, and they tended to contain a combination of local texture patterns. However, bad-condition images have the tendency to show increasingly strong disturbances with low image-frequency components such that they are observed in wide areas but are biased in location (See Figure 2 and Figure 5). In summary, the variances of color and intensity of bad-condition images are much higher than those of good-condition images. Considering low-level image processing, the image variances in Dataset-1 is limited, and accordingly the data augmentation improved the performance significantly with the production of different local images (note that CNN obtained local image features). Moreover, the diagnostic performance for bad-condition images improved in both datasets with image rotation and flipping; however, no improvement was observed for image shifting. With these augmentation procedures, we contemplate that the effects of the abovementioned strong and eccentrically located disturbances are normalized in their location when the characteristics of symptoms are emphasized. In other words, they can be said to reduce overfitting.

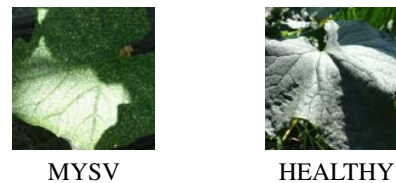


Figure 5. Example of images CNN-2 diagnosed correctly, but CNN-1 misdiagnosed

Table I
SUMMARY OF DIAGNOSTIC PERFORMANCE FOR DIFFERENT IMAGE CONDITIONS

	CNN-1[%]		CNN-2[%]		ALL
	Good-condition images	Bad-condition images [†]	Good-condition images	Bad-condition images	
Accuracy	83.2	66.9	81.6	83.0	82.3
Sensitivity MYSV	85.4	68.1	83.0	87.6	85.3
Sensitivity ZYMV	79.3	72.7	70.4	84.6	77.5
Sensitivity CCYV	92.5	81.0	89.6	89.6	89.6
Sensitivity CMV	67.8	66.9	87.8	87.8	87.8
Sensitivity PRSV	79.9	50.5	85.2	65.2	75.2
Sensitivity WMV	81.5	58.4	65.6	73.6	69.6
Sensitivity KGMMV	77.5	59.4	79.7	69.1	74.4
Specificity	91.0	70.2	90.5	94.8	92.6

[†] in Dataset-2

Table II
SUMMARY OF DIAGNOSTIC PERFORMANCE OF DIFFERENT DATA AUGMENTATIONS

Data augmentation	CNN-1[%]		CNN-2[%]		ALL
	Good-condition images	Bad-condition images	Good-condition images	Bad-condition images	
Rotation	77.4	58.8	82.4	78.0	80.2
Rotation+Mirroring	81.1	66.1	81.0	82.6	81.8
Rotation+Mirroring+Shifting	83.2	66.9	81.6	83.0	82.3

Image shifting process shows slight improvement because it generates similar patterns for CNNs (i.e., shifted images makes similar effects in the convolution process) than mirroring or rotation. Based on the assumption that symptoms are correctly captured in images, we expect CNNs detect and identify them even if the images were photographed in different conditions (e.g., taken from a distance or at close proximity) and were not seen in their training. We will investigate this carefully in our future study.

Note that all the data augmentation procedures slightly affected good-condition images obtained through CNN-2. As Dataset-2 has wide variety of images, only the image rotation process produces enough training patterns for good-condition images. Considering the best performance of CNN-1, we also assume this can be experimental upper bound in the current setting. If we seek more performance, we must introduce additional approaches to obtain more features for efficient diagnosis.

The experiments confirmed that our methodology has the potential to become a practical application. In the near future, we will develop a system capable of diagnosing physiological disorders and diseases caused from other causes such as molds and bacterium.

V. CONCLUSION

In this paper, we proposed a robust diagnostic system for cucumber viral diseases. Our system covers almost all possible viral diseases for cucumber and imposes less diagnostic restrictions during image acquisition. Our CNNs classifier attained an average of 82.3% accuracy with the 4-fold cross validation strategy.

ACKNOWLEDGMENT

This research was partially supported by Japan Science and Technology Agency (JST) (A-STEP Feasibility Study program, MP27215668083, 2016-2017).

REFERENCES

[1] E. C Oerke, H. W Dehne, "Safeguarding production losses in major crops and the role of crop protection," *Crop Protection*, Vol.23, Issue 4, pp. 275-285, 2004.

[2] J. D Pujari et al. "Recognition and Classification of Produce Affected by Identically, Looking Powdery Mildew Disease," *Acta Technologica Agriculturae*, Vol.17, Issue2, pp. 29-34, 2014.

[3] Q. Yao et al. "Application of support vector machine for detecting rice diseases using shape and color texture features," *International Conference on Engineering and Computation*, pp. 79-83, 2009.

[4] S. P Patil, R. S Zambre, "Classification of Cotton Leaf Spot Disease Using Support Vector Machine," *Journal of Engineering Research and Applications*, ISSN : 2248-9622, Vol. 4, Issue 5, Version 1, pp.92-97, 2014.

[5] D. M Mathews, "Optimizing detection and management of virus diseases of plants," *Proceedings of the Landscape Disease Symposium*, pp.10-20, 2010.

[6] B. Li et al. "Rapid,automated detection of stem canker symptoms in woody perennials using artificial neural network analysis," *Plant Methods*, Vol. 11 , 2015.

[7] H. Wang et al. "Image recognition of plant diseases based on principal component analysis and neural networks," *International Conference on Natural Computation*, pp.246-251, 2012.

[8] A. Krizhevsky et al. "ImageNet Classification with Deep Convolutional Neural Networks," *Advances In Neural Information Processing Systems*, Vol.25, pp.1106-1114, 2012.

[9] D. P Hughes, M. Salathe, "An open access repository of images on plant health to enable the development of mobile disease diagnostics," *CoRR*, abs/1511.08060, 2015.

[10] S. P Mohanty et al. "Using Deep Learning for Image-Based Plant Disease Detection," *CoRR*, abs/1604.03169, 2016.

[11] Y. Kawasaki et al. "Basic Study of Automated Diagnosis of Viral Plant Diseases Using Convolutional Neural Networks," *Lectures Notes in Computer Science*, Vol.9475, pp.638-645, 2015.

[12] FAOSTAT <http://faostat.fao.org/>

[13] Y. Gong et al. "Multi-scale Orderless Pooling of Deep Convolutional Activation Features," *CoRR*, abs/1403.1840, 2014.

[14] A. Dosovitskiy et al. "Discriminative Unsupervised Feature Learning with Convolutional Neural Networks," *CoRR*, abs/1406.6909, 2014.

[15] K. Simonyan, A. Zisserman, "Very Deep Convolutional Networks for Large-Scale Image Recognition", *CoRR*, abs/1409.1556,2014.

[16] Y. Jia et al. "Caffe: Convolutional Architecture for Fast Feature Embedding," *arXiv preprint arXiv:1408.5093*, 2014.